Spectroscopic characteristics of Er^{3+} in the two crystallographic sites of Gd_2SiO_5

2002 J. Phys.: Condens. Matter 14 3353

(http://iopscience.iop.org/0953-8984/14/12/320)

INSTITUTE OF PHYSICS PUBLISHING JOURNAL OF PHYSICS: CONDENSED MATTER

J. Phys.: Condens. Matter **14** (2002) 3353–3363 PII: S0953-8984(02)30311-4

Spectroscopic characteristics of Er^{3+} in the two crystallographic sites of Gd_2SiO_5

A S S de Camargo[1,3], **M R Davolos**[1] **and L A O Nunes**[2]

[1] Instituto de Química de Araraquara, Universidade Estadual Paulista, UNESP Av. Prof. Francisco Degni s/n, Araraquara-SP 14801-900, Brazil
[2]Instituto de Física de São Carlos, Universidade de São Paulo, USP C P 369, São Carlos-SP, 13566-590, Brazil

E-mail: andreasc@if.sc.usp.br

Received 31 October 2001
Published 15 March 2002
Online at stacks.iop.org/JPhysCM/14/3353

Abstract

Gd_2SiO_5 is among the interesting and suitable hosts for Er^{3+} which find extensive applications in the infrared, visible and ultraviolet spectral regions. In order to investigate its potentialities, a prior study of the spectroscopic behaviour of Er^{3+} substituting for Gd^{3+} ions in the two crystallographic sites of the host was performed. Absorption, excitation, site-selective emission and time-resolved spectroscopies were employed in the visible spectral region to study transitions between excited $^4S_{3/2}$ and ground $^4I_{15/2}$ states. These levels multiplets were attributed to each site separately, and their corresponding $^4S_{3/2}$ lifetimes (1.8 ± 0.1 μs for site 1 and 3.2 ± 0.1 μs for site 2) were determined.

1. Introduction

In recent years much interest has been shown in the optical properties of trivalent erbium as an impurity ion in solid hosts. The resulting materials find applications in the near-infrared, visible and ultraviolet spectral regions as laser active media at 1.5 and 2.7 μm, detectors which operate by infrared-to-visible upconversion processes and amplifying devices [1–5]. The vast potential for applications has motivated researchers to search for new and appropriate crystalline or vitreous hosts in which the spectroscopic characteristics of Er^{3+} can be explored. Among the potential hosts that can be employed, there are some rare-earth silicates [6, 7]. Single crystals of Y_2SiO_5 (YSO) for instance, have been investigated and results single this material out as a promising candidate for 1.5 μm laser action, of great interest in telecommunications [8, 9].

Gadolinium oxyorthosilicate, Gd_2SiO_5, hereafter called GSO, is a well known silicate that has been studied as a host for Tb^{3+}, Eu^{3+}, Pr^{3+} and especially Ce^{3+} ions, with applications as phosphors, on x-ray intensifying screens, in scintillating devices etc [10–14]. Its crystal

[3] Author to whom any correspondence should be addressed.

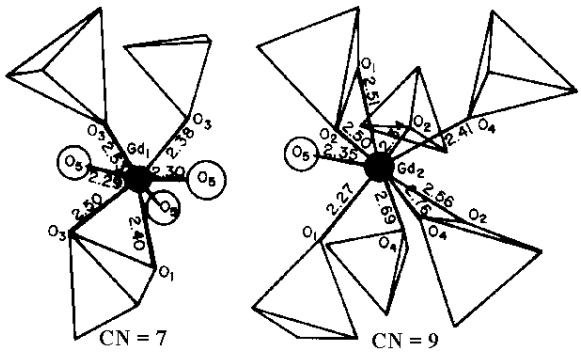

Figure 1. Crystallographic sites of monoclinic Gd_2SiO_5, space group $P2_1/c$, and corresponding interatomic distances. In both sites, Gd^{3+} ions (Gd_1 and Gd_2) are represented by a full circle at the centre of the structure. O_1, O_2, O_3 and O_4 are the O^{2-} ions bonded to the tetrahedral silicate groups and the O_5 are the isolated O^{2-} ions [16].

structure and transparency in the infrared and visible regions also allow the hosting of Er^{3+} ions and the study of its most interesting f–f transitions. Therefore, like YSO:Er^{3+}, GSO:Er^{3+} might also constitute an efficient material for applications such as those cited before, and, to the best of our knowledge, it has not been reported on yet.

One of the reasons that rare-earth silicates are interesting as hosts lies in the fact that in these compounds, the impurity ion can substitute for cations occupying low symmetry sites, especially non-inversion ones, thus increasing the oscillator strengths of transitions and consequently providing larger cross sections [15]. Also, considering that the 1.5 μm laser emission ($^4I_{13/2} \rightarrow {}^4I_{15/2}$ transition), is usually achieved by diode pumping higher-lying $^4I_{11/2}$ level at 980 nm, it is of interest to diminish upconversion and excited-state absorption losses originating at this level, so that the rate of phonon-assisted decay from $^4I_{11/2}$ to $^4I_{13/2}$ is enhanced. This can be achieved using hosts with high effective phonon energy ($\sim$1000 cm^{-1}), as is usual for several silicates due to the vibration modes of Si–O bonds [6].

The crystal structure of GSO is similar to that of YSO. According to Felsche [16], GSO is monoclinic, with spatial group $P2_1/c$, and it presents two sites in which gadolinium ions are coordinated by seven and nine oxygen ions respectively. As an impurity, Er^{3+} substitutes for Gd^{3+} in the two sites with equal or nearly equal probabilities and because these ions have similar ionic radii, for these coordination numbers [17], there should not be very significant distortions of the microstructures. Figure 1 shows the two crystallographic site structures and their corresponding interatomic distances. In a site with coordination number (CN) 7, the Gd^{3+} ion (Gd_1), is bonded to three isolated oxygen ions (O_5), and to three SiO_4^{4-} ions through two oxygen atoms in one case and through one oxygen atom in two cases. The average Gd–O distance is 2.39 Å, which is shorter than the distance by which the oxygen ions are isolated. A site with CN = 9 contains the Gd^{3+} ion (Gd_2) bonded to one isolated oxygen ion (O_5), and to six tetrahedral SiO_4^{4-} ions through two oxygen atoms in two cases and through one oxygen atom in four cases. The average Gd–O bond distance is 2.49 Å [16].

When inserted in a host like GSO, Er^{3+} ions (electronic configuration $4f^{11}$) have their free-ion energy levels split by the crystal field into $J + 1/2$ *Stark* components for each site and, assuming that Er^{3+} occupies both sites with equal or nearly equal probabilities, this number is doubled; therefore, the absorption and emission spectra of GSO:Er^{3+} can become very complex to analyse due to a large number of lines. The aim of this work was to analyse these spectra, as well as the excitation and time-resolved emission ones, in order to characterize the

spectroscopic behaviour of Er^{3+} as a function of different chemical environments—that is, in both sites. For simplicity, we limited our studies to the transitions between $^4S_{3/2}$ and $^4I_{15/2}$ states, whose energy difference lies in the green region of the spectrum, and from the results it was possible to classify the observed lines into two independent sets of levels attributed to the two sites, and also to obtain their $^4S_{3/2}$ lifetimes.

It is worth noting how powerful a tool site-selective spectroscopy has proved to be in the study of multisite systems. Several authors have reported its use to investigate and identify different sites in a great variety of systems [18–20]. In this work, the association of this technique with optical absorption, excitation and time-resolved spectroscopy resulted in a very efficient methodology for studying the optical characteristics of Er^{3+} in the two sites of GSO.

2. Experimental details

Er^{3+}-doped GSO polycrystalline samples were obtained by solid-state reaction of recently obtained Gd_2O_3:Er^{3+}, with non-crystalline SiO_2, at 1450 °C in two steps of 15 h each [10]. The starting materials were 99.99% Gd_2O_3 and Er_2O_3 from Aldrich Chem. Corp. and Alpha Products respectively, and SiO_2 60-HR, a Merck product. The doped samples studied in this work were obtained with 0.1 and 2.0 mol% Er^{3+}. The crystalline structure of the samples was verified at room temperature, by x-ray powder diffraction (XRD), using a SIEMENS D-5000 diffractometer over the range of 4°–70°, in steps of 0.02° and with an acquisition time of 5.5 s, using Cu Kα radiation at 1.5406 nm, and by vibrational absorption spectroscopy in the range of 4000–400 cm^{-1} in a Nicolet Magna IR-850 spectrophotometer with 4.0 cm^{-1} resolution, equipped with a DTGS detector and KBr beam splitter.

To obtain optical absorption spectra at room temperature and at 5 K, samples were diluted in KBr pellets which were placed in the Nicolet spectrophotometer equipped with a quartz beam splitter and a Si detector with resolution of 1.0 cm^{-1}. For the 5 K measurements, pellets were clamped to the copper cold finger of a cryostat, adapted to the equipment, and cooled by contact using a continuum liquid helium flux system ST-100 from Janis Research Co. Excitation and emission with and without selective excitation were all performed at 5 K, using the cooling system described above, except that, for these experiments, samples were analysed in the form of sintered compacts, which were excited by a Spectra Physics 375 tunable dye laser pumped by an INNOVA 400 CR argon-ion laser (the dye used was Coumarin 540 from Exciton). The sample luminescence was filtered by a 0.85 m SPEX 1403 double monochromator and collected by an RCA 31034 photomultiplier tube. Finally, time-resolved emission spectra were also obtained at 5 K using as the excitation source a dye laser, model DLM-120, pumped by a pulsed N_2 laser model VSL-337 ND from Laser Science (the dye used was again Coumarin 540). The emission pulses were collected by a 0.6 m SPEX 1877 triple monochromator, equipped with an EG&G PAR 1460 OMA multichannel detector (Diode Array), with 1024 channels.

3. Results and discussion

3.1. X-ray powder diffraction

Comparison of d_{hkl} peak values and their corresponding relative intensities extracted from the slow-paced diffraction patterns with those reported in the literature [21] indicated that the formation of the monoclinic structure of GSO was achieved in all samples.

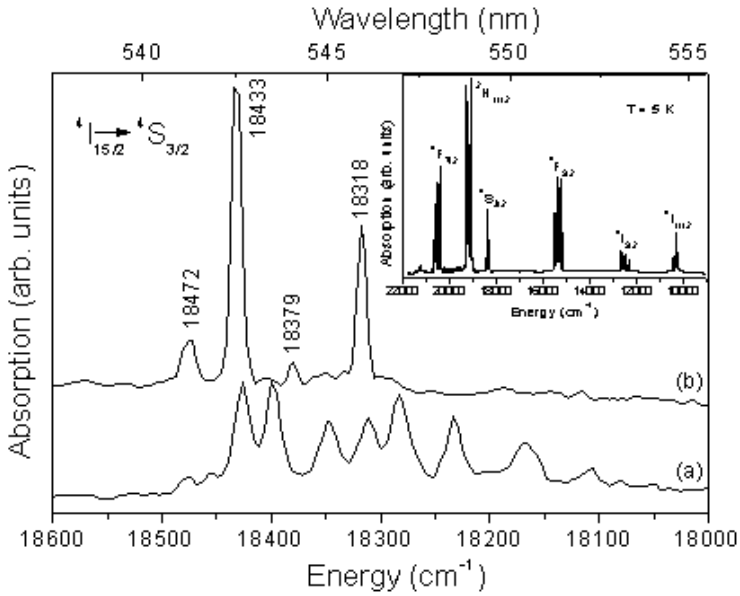

Figure 2. An enlargement of the GSO:Er^{3+}(0.1%) optical absorption spectrum obtained at (a) $T = 300$ K and (b) $T = 5$ K, in the region of the $^4I_{15/2} \rightarrow {}^4S_{3/2}$ transition. The inset illustrates the original spectrum at $T = 5$ K in which spectral lines correspond to transitions from the ground to the excited states indicated.

3.2. Vibrational absorption

The analysis of samples by vibrational absorption also indicated the formation of monoclinic GSO. The transmittance spectra were practically identical, presenting typical bands which were attributed according to Lazarev [22]. There is a triply degenerate band around 900 cm^{-1} corresponding to vibrations due to asymmetric stretching (ν_{as}) of Si–O bonds, characteristic of silicate groups, and also bands in the range of 420–570 cm^{-1}, attributed to Si–O deformations (δ) or Ln–O stretching (ν).

3.3. Optical absorption spectra

The optical absorption spectra of GSO:Er^{3+}(0.1%) ($^4I_{15/2} \rightarrow {}^4S_{3/2}$ transition) obtained at room temperature (a) and at $T = 5$ K (b) are illustrated in figure 2. The inset of the figure also shows the spectrum obtained at $T = 5$ K in the larger range of 22 000–9000 cm^{-1}, in which lines corresponding to transitions from the ground $^4I_{15/2}$ to the indicated excited states can be observed. At this temperature, only the lowest sublevel of the $^4I_{15/2}$ ground state is populated and so the observed number of lines for the excited states should image their splitting. Considering the $^4S_{3/2}$ level ($J = 3/2$), there is a splitting into two sublevels (*Stark* levels), and that is in accordance with the observation of four intense lines of (b), two for each low-symmetry site, at 18 472, 18 433, 18 379 and 18 318 cm^{-1}. At $T = 300$ K, other sublevels of the ground $^4I_{15/2}$ state are thermally populated and therefore more spectral lines are observed.

Beyond the presence of four absorption lines, as expected for $T = 5$ K, spectrum (b) also displays small bumps beside the major lines, especially at around 18 350 cm^{-1}. Since the signal-to-noise ratio for this experiment was low, it is hard to establish the origin of these

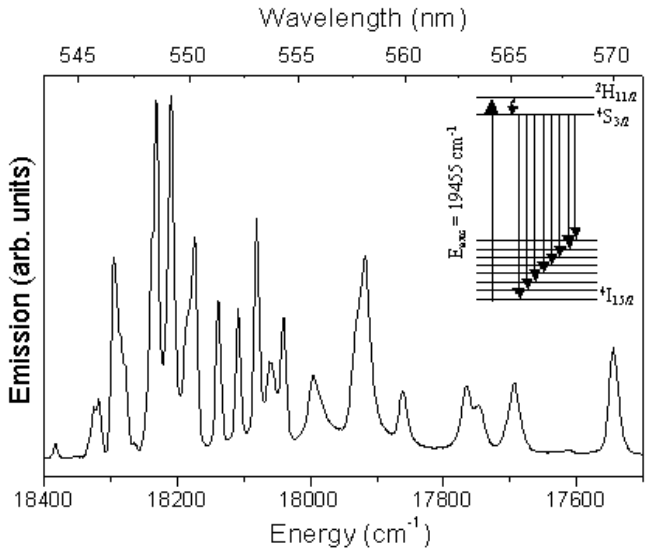

Figure 3. A GSO:Er^{3+}(0.1%) emission spectrum corresponding to the $^4S_{3/2} \rightarrow {}^4I_{15/2}$ transition, obtained at 5 K, with $E_{exc} = 19\,455$ cm^{-1} ($^2H_{11/2}$ energy level). The inset shows a schematic energy level diagram with transitions that are to be associated with the spectrum lines.

spectral features; however, their existence might suggest the presence of an impurity phase in the samples—that is, a secondary structure in such small quantity that it could not be identified in the x-ray diffraction patterns. Moreover, the attribution of the four major lines to both sites, separately, was not possible at this stage. An effective way of doing this could be by analysis of polarized absorption spectra [23, 24]; however, that could not be accomplished since the samples studied in this work are in the polycrystalline form.

3.4. Selectively excited luminescence spectra

Figure 3 presents a GSO:Er^{3+}(0.1%) luminescence spectrum ($^4S_{3/2} \rightarrow {}^4I_{15/2}$ transition), obtained by populating $^4S_{3/2}$ through the excitation of the $^2H_{11/2}$ level at 19 455 cm^{-1}. Since the spectrum was taken at $T = 5$ K, and due to the high non-radiative rate of decay from the higher- to the lower-lying $^4S_{3/2}$ sublevel, the radiative recombination occurs between the latter and the eight sublevels of the ground $^4I_{15/2}$ state as represented in the inset of the figure. Assuming that this higher energy should be responsible for the excitation of Er^{3+} ions in both sites, the observation of a total of 16 spectral lines was expected (for the two sites); however, as can be noted, the spectrum contains at least 20 lines, some quite broadened.

The occurrence of more than 16 lines once again gave rise to the hypothesis that there could be an impurity phase along with GSO in the samples, as was previously suggested by the absorption spectrum. To ensure that some of the lines were not originating from thermal population of the higher-lying $^4S_{3/2}$ sublevel, temperature-dependent spectra were investigated, but comparison with previous results did not confirm this. Also, the possibility of having cluster sites and Er^{3+}-ion pairs was considered by comparing these results with those obtained for the 2.0%-doped sample; however, as the spectra were practically identical, there was no evidence of these structures forming up to this doping concentration.

Aiming to discriminate between the lines of Er^{3+} and to attribute them to the two sites of GSO, and also to identify the origin of the extra lines observed, careful investigation by site-

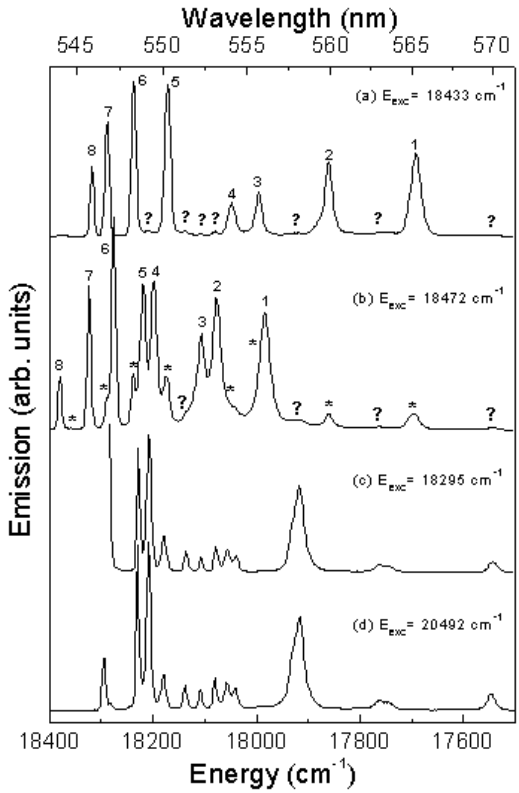

Figure 4. GSO:Er^{3+}(0.1%) emission spectra obtained at 5 K with selective excitation at: (a) 18 433 cm^{-1}; (b) 18 472 cm^{-1}; and (c) 18 295 cm^{-1}. The numbers on (a) and (b) indicate lines assigned to site 1 and site 2 respectively; question marks indicate lines corresponding to the impurity phase Gd_2O_3:Er^{3+} and the stars on (b) correspond to GSO site 1 lines. The spectrum (d) was obtained for a Gd_2O_3 sample doped with 0.1 mol% Er^{3+}, with excitation at 20 492 cm^{-1} (the 488 nm line of an Ar^+ laser).

selective spectroscopy was performed. We started by exciting the sample at the most intense absorption lines at 18 433, 18 318, 18 472 and 18 379 cm^{-1}, which were previously associated with both sites. Figure 4 trace (a) is the spectrum obtained with excitation at 18 433 cm^{-1} and, as can be noted, it contains eight intense lines (numbered), and also less intense lines indicated by question marks. Exciting the sample at 18 318 cm^{-1} led to an identical spectrum except for a small intensity variation of the lines indicated by question marks; the numbered lines, however, remained the most intense and were attributed to one of the sites, which is labelled and referred to as 'site 1' from now on. The attribution of the other eight intense lines to 'site 2' was based on the spectra obtained with excitation at 18 472 and at 18 379 cm^{-1}. Besides the site-2 lines in figure 4 spectrum (b), the lines indicated by question marks (the same as for 4 spectrum (a)) and those attributed to site 1 (indicated by stars) were also observed. The presence of lines arising from both sites in figure 4 spectrum (b) is evidence for energy transfer from site 2 to site 1, even when the former is selectively excited.

Attention should be drawn now to the unidentified lines indicated by question marks in figures 4, (a) and (b). As previously discussed, we had a tendency to attribute these lines to a secondary phase coexisting with GSO:Er^{3+} in the samples, and to study this possibility, excitation at the bumps observed in the absorption spectrum was performed. The spectrum

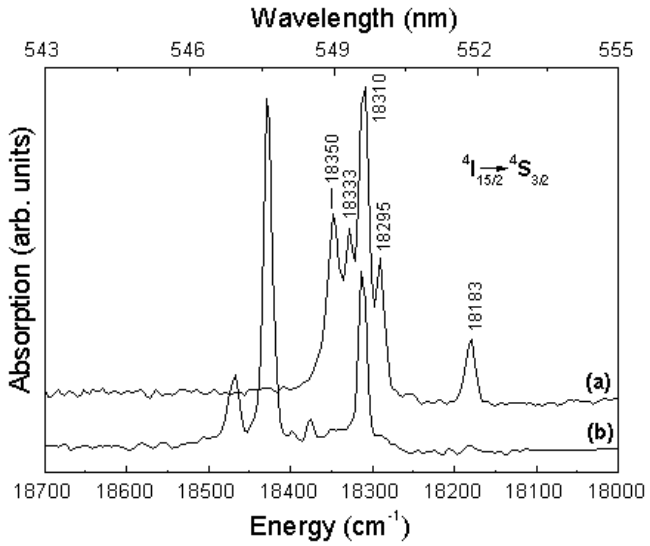

Figure 5. Optical absorption spectra obtained at $T = 5$ K and corresponding to $^4I_{15/2} \rightarrow {}^4S_{3/2}$ transition: (a) Gd_2O_3:Er^{3+}(0.1%); (b) GSO:Er^{3+}(0.1%).

obtained with $E_{exc} = 18\,295$ cm^{-1} is presented in figure 4, trace (c). As can be seen by comparison, it is composed of the same extra lines as those being investigated (and some more), which were not attributed either to site 1 nor to site 2. These lines correspond to Er^{3+} ions in two sites of monoclinic Gd_2O_3, which was used as one of the sample precursors. Proof of this is found by comparison of figure 4 trace (c) with the almost identical spectrum, figure 4 trace (d), obtained for a Gd_2O_3 sample doped with 0.1 mol% Er^{3+} with excitation at 20 492 cm^{-1}. Moreover, figure 5 trace (a) represents a Gd_2O_3:Er^{3+} absorption spectrum and, as can be noted, a total of five lines are observed at 18 350, 18 333, 18 310, 18 295 and 18 183 cm^{-1}. These results explain the observation of lines corresponding to the doped oxide when sites 1 and 2 of GSO:Er^{3+} were selectively excited (figures 4, spectra (a) and (b)). In this case, Gd_2O_3:Er^{3+} sites were also being excited by means of energy transfer from the silicate sites. Moreover, it also becomes clear why the luminescence spectrum in figure 3, obtained with excitation at higher energy, contains more lines than were expected, since it is composed by the summation of silicate lines (from both sites) and oxide lines, several of them being superposed.

The presence of some remaining Gd_2O_3:Er^{3+} in the samples is probably due to an incomplete reaction between this oxide and SiO_2. Several factors could have contributed for this: time and temperature, for instance, play a very important role in solid-state reactions; the slow diffusion of silica ought to be considered as an important factor too and, besides, due to the latter's high rate of water absorption, there could be some implications for the stoichiometry of the reaction as well.

3.5. Excitation spectroscopy

The absorption line attribution could yet be confirmed through analysis of excitation spectra obtained at $T = 5$ K, by fixing the detection of the emission lines at the lowest energy, corresponding to both sites, and varying the excitation energy. As an example, figure 6 illustrates the spectrum obtained by monitoring the intensity of the site 1 emission line at

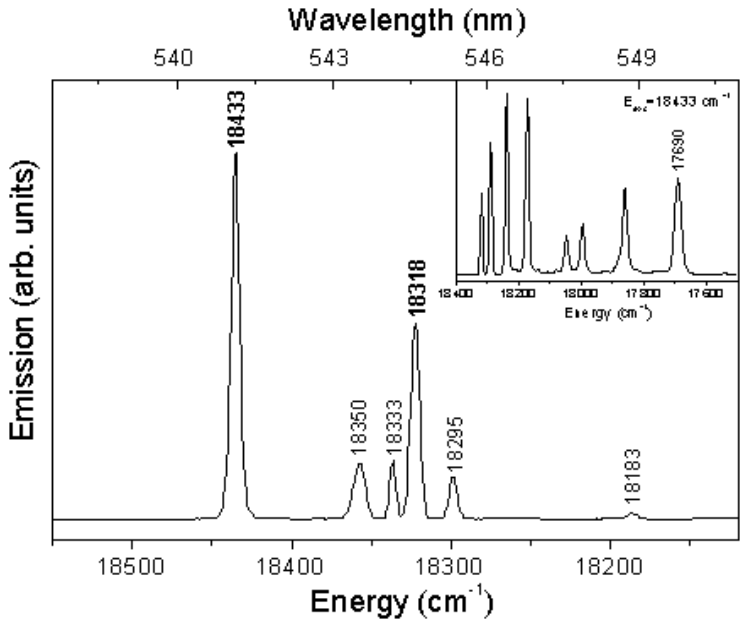

Figure 6. A GSO:Er^{3+}(0.1%) representative excitation spectrum obtained at $T = 5$ K, monitoring the emission line of site 1 at 17 690 cm^{-1}, ($^4S_{3/2} \rightarrow {}^4I_{15/2}$ transition).

17 690 cm^{-1} as indicated in the spectrum of the inset. Although the excitation spectrum presents a total of six lines, it is easy to see that the lines at 18 433 and 18 318 cm^{-1} which were previously attributed to GSO:Er^{3+} site 1 are at least three times more intense than the others. In accordance with previous results, the four lines at 18 350, 18 333, 18 295 and 18 183 cm^{-1} correspond to the three sites of monoclinic Gd_2O_3:Er^{3+} (figure 5 trace (a)), and by examining GSO:Er^{3+} absorption spectrum again (figure 5 trace (b)), it is also possible to observe their presence in the form of bumps. The coexistence of oxide and silicate lines in the excitation spectrum of figure 6 reflects the oxide's contribution to the luminescence of GSO:Er^{3+}; that is, there are processes of energy transfer from the oxide to the silicate which are favoured by the longer $^4S_{3/2}$ lifetimes of the oxide (of about 18 μs). Analogous measurements were performed for site 2, confirming the attribution of lines at 18 472 and 18 379 cm^{-1} as well. The results for sites 1 and 2 are summarized in table 1.

3.6. Time-resolved emission spectra

Considering that the sites' different chemical environments would affect their $^4S_{3/2}$-state lifetimes, time-resolved emission spectra were investigated in an attempt to determine them and also to distinguish, in time, the lines corresponding to each site. Figure 7 illustrates the time-integrated spectra obtained at $T = 5$ K with $E_{exc} = 18\,433$ cm^{-1} (trace (a)); and with $E_{exc} = 18\,472$ cm^{-1} ((b) and (c)). Spectrum (a) was obtained with no detection delay and it presents the emission lines corresponding to site 1 as previously discussed. Spectrum (b) was also obtained without detection delay and it presents the eight lines corresponding to site 2 and, due to energy transfer, lines corresponding to site 1 are also observed (indicated by arrows). As a gate of 0.5 μs and detection delays were progressively introduced, the latter had their intensity diminished and only site 2 lines remained in the spectra, as can be noted

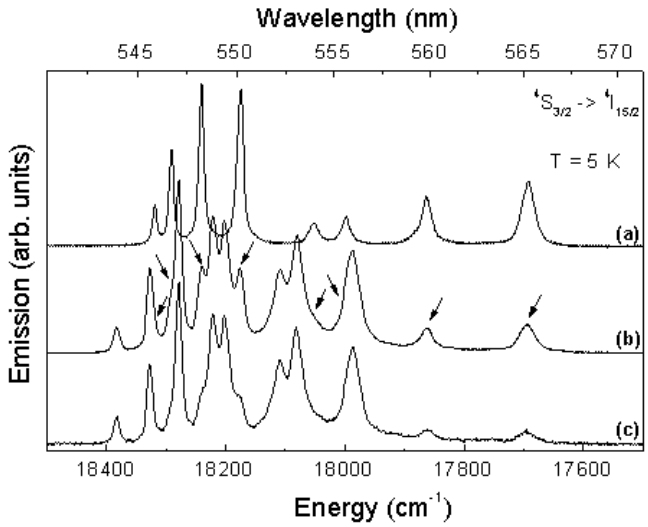

Figure 7. GSO:Er^{3+}(0.1%) time-resolved emission spectra obtained at $T = 5$ K with: $E_{exc} = 18\,433$ cm^{-1} and no detection delay (a); $E_{exc} = 18\,472$ cm^{-1} and no detection delay (b); $E_{exc} = 18\,472$ cm^{-1} with 0.5 μs gate and 5.0 μs delay (c). The arrows in (b) indicate site 1 emission lines which have their intensity diminished after the detection delay is introduced in spectrum (c).

Table 1. Experimental values of the Stark $^4I_{15/2}$ and $^4S_{3/2}$ components at 5 K and lifetime values, for GSO:Er^{3+}(0.1 mol%); site 1 (column 2), and site 2 (column 3).

Energy level	Site 1 (CN = 7) (cm^{-1})	Site 2 (CN = 9) (cm^{-1})
$^4S_{3/2}$	18 433	18 472
	18 318	18 379
$^4I_{15/2}$	628	385
	458	303
	320	275
	270	181
	146	163
	80	105
	30	57
	0	0
	$\tau = 1.8 \pm 0.1$ μs	$\tau = 3.2 \pm 0.1$ μs

in spectrum (c) in figure 7, obtained after a 5.0 μs delay. Such observation implies that site 1 has a shorter $^4S_{3/2}$ lifetime value than site 2 and consequently it is not possible to isolate its lines by exciting the sample with energies other than those of its absorption bands at 18 433 and 18 318 cm^{-1}. From linear fits of the intensity decay curves of each line corresponding to the two sites as a function of the detection delays, it was possible to obtain the average $^4S_{3/2}$ lifetimes of: 1.8 ± 0.1 μs with a correlation coefficient $R = 0.99$ for site 1; and 3.2 ± 0.1 μs ($R = 0.99$) for site 2.

Taking account for the existence of energy-transfer processes among the sites, they should be strongly favoured by a high concentration of doping ions and, in this case, the transfer could have an effect on the intensity decay profiles. Indeed, although the emission spectra for the

samples doped with 0.1 and 2.0 mol% Er^{3+} are identical as regards the number, position and relative intensity of the lines, the sample doped with 2.0% presents shorter lifetime values (1.5 ± 0.1 μs for site 1 and 2.8 ± 0.1 μs for site 2). The reason for this is a smaller distance and therefore higher interaction between Er^{3+} ions favouring energy transfer, which constitutes a novel way of depopulating $^4S_{3/2}$ non-radiatively.

Assuming a single-exponential decay is pretty reasonable even though that would be, at first, inconsistent with the occurrence of energy transfer even for low (0.1%) doping concentration. This contradiction is only apparent because these processes happen on a timescale much shorter than that of the radiative processes in which we were interested and, also, they could not be observed through the method used. To investigate the transfer itself, it would be necessary to use *nanosecond*-order gates, which was not viable for the detection of the low-intensity signal observed. The energy transfer in this system is favoured by the position of $^4S_{3/2}$ sublevels for both sites on the energy scale. Because site 2 sublevels are located at higher energy, site 1 sublevels can be populated by a process of relaxation from site 2. The reverse transfer (from site 1 to site 2) is not observed, probably due to the shorter lifetime and consequently higher radiative transition probability observed for site 1.

The spectroscopic characteristics of Er^{3+} can be correlated with the site microstructures. It seems reasonable to expect the interaction between an Er^{3+} ion and an isolated O^{2-} to be stronger than that between an Er^{3+} and oxygen ions belonging to silicate groups, especially if their interatomic distances are short. Considering the average interatomic distances (2.39 Å for a site with CN = 7 and 2.49 Å for a site with CN = 9) and the number of isolated O^{2-} bonded to Er^{3+} (three for CN = 7 and one for CN = 9), the site with CN = 7 should present higher orbital interaction than the site with CN = 9 [11]. The higher orbital interaction favours transition probabilities and consequently shorter lifetimes are observed. Therefore, experimental results led us to assign coordinations 7 and 9 to sites 1 and 2 respectively, as presented in table 1. This assignment is in accordance with that for GSO:Eu^{3+}; that is, the average lifetime value of the $Eu^{3+5}D_0$ state in site 1 (CN = 7) is 1.7 ms and for site 2 (CN = 9) it is 2.1 ms [10]. Therefore, both Eu^{3+} and Er^{3+} ions present shorter lifetime values when the ion occupies site 1.

4. Conclusions

The spectroscopic characteristics of Er^{3+} in the two crystallographic sites of Gd_2SiO_5 were studied. By association of absorption, excitation, site-selective emission and time-resolved spectroscopies it was possible to assign spectral lines corresponding to *Stark* components of ground $^4I_{15/2}$ and excited $^4S_{3/2}$ states and to determine lifetimes for Er^{3+} ions inserted in site 1 and in site 2, based on the site microstructures. Site 1, with shorter bond distances, larger crystal-field splitting and a lifetime of 1.8 ± 0.1 μs (for the 0.1%-doped sample), was identified as the site with CN = 7 and local C_s symmetry. Site 2, with longer bond distances, smaller energy level splittings and lifetime 3.2 ± 0.1 μs, was identified as the site with CN = 9 and approximate C_{3v} symmetry.

Acknowledgments

This work was financially supported by Capes (*Coordenação de Aperfeiçoamento de Pessoal de Nível Superior*), CNPq (*Conselho Nacional de Desenvolvimento Científico e Tecnológico*) and FAPESP (*Fundação de Amparo à Pesquisa do Estado de São Paulo*). A S S de Camargo is especially grateful to Capes for a Masters course fellowship.

References

[1] Taccheo S, Laporta P and Svelto O 1996 *Appl. Phys. Lett.* **69** 3128
[2] Jouart J P and Mary G 1990 *J. Lumin.* **46** 39
[3] Esterowitz L, Hoffman C A, Tran D C, Levin K, Storm M, Bonner R F, Smith P and Leon M 1986 *SPIE Proc. Opt. Laser Technol. Med.* **605** 32
[4] Silversmith A J, Lenth W and MacFarlane R N 1987 *Appl. Phys. Lett.* **51** 1977
[5] Hirao K, Todoroki S and Sogan N J 1992 *J. Non-Cryst. Solids* **143** 40
[6] Fornasiero L, Petermann K, Heumann E and Huber G 1998 *Opt. Mater.* **10** 9
[7] Souriau J C, Romero R, Borel C, Wyon Ch, Li C and Moncorgé R 1994 *Opt. Mater.* **4** 133
[8] Doualan J L, Labbé C, Le Boulanger P, Margerie J, Moncorgé R and Timonen H 1995 *J. Phys.: Condens. Matter* **7** 5111
[9] Li C, Moncorgé R, Souriau J C, Borel C and Wyon Ch 1994 *Opt. Commun.* **107** 61
[10] Simoneti J A 1996 *Thesis* Universidade Estadual Paulista, UNESP, Brazil
[11] Lammers M J J and Blasse G 1987 *J. Electrochem. Soc.* **134** 2068
[12] Hölsä J, Jyrkäs K and Leskelä M 1986 *J. Less-Common Met.* **126** 215
[13] Ishibashi H, Kurashige K, Kurata Y, Susa K, Kobayashi M, Tanaka M, Hara K and Ishii M 1998 *IEEE Trans. Nucl. Sci.* **45** 518
[14] Kuleshov N V, Shcherbitsky V G, Lagatsky A A, Mikhailov V P, Minkov B I, Danger T, Sandrock T and Huber G 1997 *J. Lumin.* **71** 27
[15] Li C, Lagriffoul A, Moncorgé R, Souriau J C, Borel C and Wyon Ch 1994 *J. Lumin.* **62** 157
[16] Felsche J 1973 *Struct. Bonding* **13** 99
[17] Shannon R D 1976 *Acta Crystallogr.* A **32** 751
[18] Cockroft N J, Thompson D, Jones G D and Symes R W G 1987 *J. Chem. Phys.* **86** 521
[19] Goldner Ph and Pellé F 1993 *J. Lumin.* **55** 197
[20] Dierolf V, Kutsenko A B, Sandmann C, Tröster Th and Corradi G 2000 *J. Lumin.* **87** 989
[21] *JCPDS file number 40-0287* JCPDS International Center for Diffraction Data
[22] Lazarev A N 1972 Vibrational Spectra and Structure of Silicates (New York: Consultants Bureau) p 302
[23] Witte O, Stolz H and von der Osten W 1996 *J. Phys. D: Appl. Phys.* **29** 561
[24] Gruber J B, Quagliano J R, Reid M F, Richardson F S, Hills M E, Seltzer M D, Stevens S B, Morrison C A and Allik T H 1993 *Phys. Rev.* B **48** 15 561